



An isotopic analysis of ionising radiation as a source of sulphuric acid

M. B. Enghoff¹, N. Bork^{1,2,4}, S. Hattori³, C. Meusinger⁴, M. Nakagawa⁵, J. O. P. Pedersen¹, S. Danielache^{3,6}, Y. Ueno⁶, M. S. Johnson⁴, N. Yoshida^{3,5}, and H. Svensmark¹

¹National Space Institute, Technical University of Denmark, 2100, Copenhagen Ø, Denmark

²Division of Atmospheric Science, Department of Physics, P.O. Box 64, 00014 University of Helsinki, Finland

³Department of Environmental Science and Technology, Interdisciplinary Graduate School of Science and Engineering, Tokyo Institute of Technology, Yokohama, 226-8502, Japan

⁴University of Copenhagen, Department of Chemistry, 2100, Copenhagen Ø, Denmark

⁵Department of Environmental Chemistry and Engineering, Interdisciplinary Graduate School of Science and Engineering, Tokyo Institute of Technology, Yokohama, 226-8502, Japan

⁶Department of Earth and Planetary Science, Tokyo Institute of Technology, Meguro-ku, Tokyo, 152-8551, Japan

Correspondence to: M. B. Enghoff (enghoff@space.dtu.dk)

Received: 17 November 2011 – Published in Atmos. Chem. Phys. Discuss.: 13 February 2012

Revised: 24 May 2012 – Accepted: 2 June 2012 – Published: 19 June 2012

Abstract. Sulphuric acid is an important factor in aerosol nucleation and growth. It has been shown that ions enhance the formation of sulphuric acid aerosols, but the exact mechanism has remained undetermined. Furthermore some studies have found a deficiency in the sulphuric acid budget, suggesting a missing source. In this study the production of sulphuric acid from SO₂ through a number of different pathways is investigated. The production methods are standard gas phase oxidation by OH radicals produced by ozone photolysis with UV light, liquid phase oxidation by ozone, and gas phase oxidation initiated by gamma rays. The distributions of stable sulphur isotopes in the products and substrate were measured using isotope ratio mass spectrometry. All methods produced sulphate enriched in ³⁴S and we find an enrichment factor ($\delta^{34}\text{S}$) of $8.7 \pm 0.4\%$ (1 standard deviation) for the UV-initiated OH reaction. Only UV light (Hg emission at 253.65 nm) produced a clear non-mass-dependent excess of ³³S. The pattern of isotopic enrichment produced by gamma rays is similar, but not equal, to that produced by aqueous oxidation of SO₂ by ozone. This, combined with the relative yields of the experiments, suggests a mechanism in which ionising radiation may lead to hydrated ion clusters that serve as nanoreactors for S(IV) to S(VI) conversion.

1 Introduction

Aerosols – small particles suspended in air – are frequently formed by condensation of gas molecules in Earth's atmosphere. The effect of these particles on the radiative balance of our climate system, through direct and indirect mechanisms, is the greatest uncertainty in the radiative forcing budget (Forster et al., 2007). One issue is that the mechanism behind the formation of aerosols remains unknown, even though several mechanisms have been proposed (Kulmala, 2003; Curtius, 2006; Kurtén et al., 2008) and major advances have recently been made (Kirkby et al., 2011). One of these mechanisms is that of ion-induced nucleation (Enghoff and Svensmark, 2008; Kazil et al., 2008; Hirsikko et al., 2011) where ionising radiation promotes the early stages of the aerosol nucleation. The prevailing theory on exactly how the ions affect nucleation is that they lower the energy barrier for condensing molecules caused by the increase in energy required to create the interface between the aerosol phase and the gas phase – the surface tension (Lovejoy et al., 2004). Other factors include the recombination of oppositely charged clusters (Yu and Turco, 2000) and the increased growth rate caused by a charge in a molecular cluster (Yu and Turco, 2001). Ionic cluster formation is estimated to account for 1–30% of total particle formation, based on 7 European

measurement sites (Manninen et al., 2010) and ionisation by galactic cosmic rays may increase binary (sulphuric acid and water) and ternary (sulphuric acid, water, ammonia) nucleation rates of nanometer size particles in the tropospheric boundary layer (Kirkby et al., 2011). Svensmark et al. (2007) proposed a chemical mechanism where sulphuric acid is produced by ion chemistry, but until now there has been no experimental evidence supporting this mechanism.

Sulphuric acid is thought to be one of the main components of aerosols nucleated in the atmosphere (Sipilä et al., 2010) and an extra source might therefore be important for understanding aerosol formation. During a measurement campaign in Hyytiälä, Finland the calculated sulphuric acid concentrations were about 10 percent lower than the measured values (Boy et al., 2005), and a study at the Antarctic also showed a missing sulphuric acid source (Jefferson et al., 1998) stimulating the search for possible additional sources of sulphate. An ion mechanism could additionally operate at night, providing a source of sulphuric acid not depending on sunlight.

The initial steps of a mechanism involving ion chemistry have been investigated by e.g. Fehsenfeld and Ferguson (1974) and more recently by Bork et al. (2011a,b) who used ab initio calculations to show that the gas-phase oxidation of SO₂ by ozone is facilitated in ionic clusters, but until now there has been no direct experimental investigation. One of the difficulties of such a study is that nucleation requires a certain amount of condensable gas and thus either a liquid or photochemical source of sulphuric acid is normally used (Berndt et al., 2006). Any effect from an ionising source then occurs in parallel with this other source and is thus hard to distinguish. An early study by Raes et al. (1985) showed an increase in particle number when a gamma source was used in addition to photochemical sulphuric acid production and they speculated that both UV light and gamma rays could produce sulphuric acid from SO₂.

An alternative technique for distinguishing in situ processes is isotopic analysis. Fractionating processes alter the isotopic composition of chemical species and are used to constrain atmospheric budgets or interpret geological records and ice cores, e.g. Johnson et al. (2002); Brenninkmeijer et al. (2003). Traditional physical processes and most chemical reactions follow a so-called mass-dependent relationship (MDF, mass-dependent fractionation), where enrichments of different isotopes follow a linear relationship according to the ratio of their masses. A deviation from the linear behavior is sometimes observed, but the origin(s) of non-mass-dependent fractionation, abbreviated NMD, is not fully understood. NMD is, however, known to be produced by a small number of mechanisms occurring in the gas phase including photolysis and recombination reactions, as well as some nuclear processes (Guo et al., 2010; Romero and Thiemens, 2003; Thiemens, 2006). Photolytic reactions can result in NMD due to differences in absorption cross sections caused

by isotopic substitution (Danielache et al., 2008; Schmidt et al., 2011).

Sulphur has four stable isotopes (³²S, ³³S, ³⁴S, and ³⁶S) and is widely used for isotopic analysis. It is known that the photolytic fractionation of sulphur compounds is wavelength dependent (Farquhar et al., 2000b) and another possible source for NMD is the oxidation channel of excited SO₂, a process very likely to happen in the atmosphere. NMD signatures have been found in atmospheric sulphate aerosols (Baroni et al., 2007; Pavlov et al., 2008) and Archean rock samples (Farquhar et al., 2000a; Ono et al., 2003; Ueno et al., 2008; Bao et al., 2007). In a previous study, Harris et al. (2012) investigated different gas and liquid phase oxidation pathways of SO₂ in laboratory experiments, but did not observe clear NMD with respect to ³³S, while the sulphate production processes under consideration were generally distinguishable by their ³⁴S fractionation factors.

While the isotopic fractionations of SO₂ by ionising radiation are not known, NMD is not expected. From the Born-Oppenheimer approximation it is evident that molecular polarizability is not changed by isotopic substitution. In particular the S in SO₂ is at a symmetric site and it has previously been shown, for ozone, that NMD effects are primarily associated with asymmetric sites (e.g. the two end atoms in ozone) but not at symmetric sites, such as the central atom in ozone (Gao and Marcus, 2001).

In this study we generate sulphuric acid using UV light, gamma sources, and via ozone oxidation in the aqueous phase. Using multiple sulphur isotopic measurements allows us to distinguish between these reactions and evaluate their relative importance.

2 Experimental setup and procedures

The experiments were performed using two separate systems. Sulphuric acid was generated using a chemical reaction chamber at the National Space Institute in Copenhagen. Samples were collected as BaSO₄ by flowing the air leaving the reactor through a series of bubblers containing BaCl₂. The isotopic composition of the samples were then analysed with an isotope ratio mass spectrometer (IRMS) at the Tokyo Institute of Technology. The following sections describe each experimental system and the procedures employed.

2.1 Chamber setup (Copenhagen)

A schematic of the setup can be seen in Fig. 1. The reaction volume was contained in a cylindrical 501 reaction chamber (100 cm long with a diameter of 25 cm) made of electropolished stainless steel, previously described by Enghoff et al. (2008). A mixture of pure humidified air (Labline 5.0, Strandmøllen, further cleaned with a Thermo Scientific model 1160 Zero Air Supply) was continuously flowed through the vessel at a rate of 1.01 min⁻¹ (standard

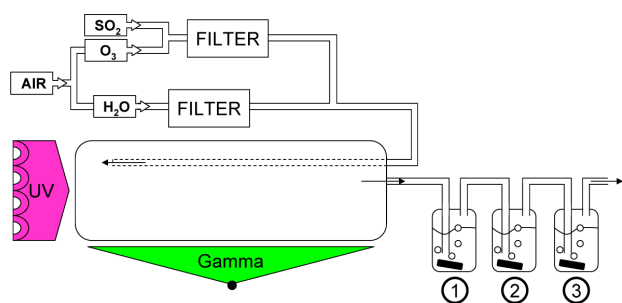


Fig. 1. Schematic of the chamber setup in Copenhagen. The purified airstream is split in two, one passing through the humidifier and the other through the ozone generator before rejoining along with the SO_2 flow and entering the chamber (see text). The airstream leaving the reaction volume is passed through 3 numbered gas washing bottles, in series, with magnetic stirrers. Collimated UV light enters through a Teflon foil at the end of the chamber, while a gamma source is placed at the side.

temperature and pressure (STP)). Previous to entering the chamber 0.41 min^{-1} of the purified air went through an ozone generator (using photolysis at 184 nm) resulting in about ~ 400 ppb ozone in the chamber. The rest of the air (0.61 min^{-1}) was humidified by circulating purified (milli-Q) water through a GoreTex tube inserted into the air stream, giving a relative humidity of 40–45 %. In addition $100 \mu\text{l min}^{-1}$ (STP) of pure $\text{SO}_2(\text{g})$ evaporated from a container (Gerling Holz+Co, ≥ 99.95 % wt.) was sent through the chamber. All air entering the chamber was additionally cleaned with a PALL Kleenpack 3 nm particle filter.

The temperature and absolute pressure was that of the laboratory, typically 22°C (with UV lamps off) and 30°C (UV on) and 1 bar, with a 1 mbar overpressure in the reaction vessel. Temperature, absolute and differential pressure, and relative humidity were monitored.

An array of UV (Philips TUV PL-L 18 W mercury discharge) lamps were used to illuminate the chamber with UV-radiation primarily at 253.65 nm (the lamp spectrum is shown in the Supplement). The lamps were placed about 20 cm from the chamber, separated by 2 layers of Teflon foil to maintain an air-tight system but transmit UV. The UV light initiates photochemistry in the gas phase, where ozone is photolysed producing excited oxygen atoms that form OH via reaction with H_2O , initiating the oxidation of SO_2 into sulphuric acid (see Appendix C).

Alternatively the chamber could be exposed to gamma radiation from two 35 MBq Cs-137 sources, placed 27 cm from the side of the chamber.

The outlet air from the chamber was connected to a series of glass gas washing bottles (typically 3) used to collect the sulphuric acid. These bottles contained 400 ml of milli-Q water adjusted to pH 2 using hydrochloric acid with an excess (1.0 g) of barium chloride ($\text{BaCl}_2(\text{H}_2\text{O})_2$) compared to the amounts of sulphate formed in the experiments (mil-

ligrams). The bottles were magnetically stirred to maximize the air-water interaction. When the sulphuric acid entered the bottles it reacted with the barium ions to form BaSO_4 which has a very low solubility in water. The pH of 2 was chosen to prevent SO_2 from the gas phase from dissolving in water forming the sulphite ion (SO_3^{2-}), which could potentially precipitate as BaSO_3 . Acidic conditions at pH 2 shift the equilibrium away from SO_3^{2-} , instead favoring aqueous SO_2 and HSO_3^- . We attempted to dissolve a small part of some of the samples with 4 M HCl. It did not dissolve, demonstrating that the product was not BaSO_3 .

All experiments ran for one week. The sample was then collected by allowing the BaSO_4 to settle, decanting the excess liquid and thoroughly resuspending the remaining solids in milli-Q water. This procedure was repeated three times for each sample to remove any remaining BaCl_2 . The remaining solution was transferred to a smaller container and the water was evaporated in an oven, leaving the BaSO_4 as a powder.

The first column of Table 1 shows the experiments used for further analysis. Five different types of experiments were done, to distinguish oxidation pathways for SO_2 . UV light and the gamma source were used separately and together. In addition, a series of experiments were run without UV and gamma source to quantify any uptake and oxidation of SO_2 in the liquid phase. Finally, an experiment was run with no UV, no gamma source, and no ozone, which did not yield any detectable amount of sulphuric acid.

The isotopic composition of the liquid SO_2 had to be determined, as a reference point for the isotopic data. About 5 ml of SO_2 (0.2 mmol) was added to a solution consisting of 500 ml milli-Q water with 15 mmol H_2O_2 , as oxidizing agent. The solution was adjusted to pH 11 before SO_2 was added to ensure dissolution. The solution was stirred overnight and $\text{BaCl}_2(\text{H}_2\text{O})_2$ was added. The resulting BaSO_4 was collected using the method described above. A second reference was prepared in the same fashion, except pH was not adjusted, in order to test for any pH dependence, even though the reaction is supposedly almost pH-independent (Seinfeld and Pandis, 2006, chap. 7). The two references yielded 41.8 and 36.7 mg of BaSO_4 , respectively, from the ~ 5 ml of SO_2 . This corresponds to 0.18 and 0.16 mmol. The collected amounts suggest full conversion of the SO_2 transferred and losses of BaSO_4 from sample collection. A small sample of the reference could not be dissolved with 4 M HCl, showing that the product was sulphate and not sulphite.

2.2 Isotope fractionation setup (Tokyo)

The collected BaSO_4 was converted to SF_6 for isotopic analysis. The first step was conversion into Ag_2S : the BaSO_4 was held at 300°C and reduced to H_2S with the modified Kiba reagent (concentrated, dehydrated phosphoric acid containing Sn^{2+} , Sakai et al., 1984). The generated H_2S was then

Table 1. *Samples and results.* The table displays a sample ID, the mass of BaSO₄ recovered, and the isotopic fractionation data (normalized against the references as defined in Appendix B). The sample ID refers to the method of sulphate production: O₃ is the liquid phase oxidation by ozone, UV is when the UV lamps were turned on, and γ is when the gamma source was used. The number at the end of the ID refers to the position of the bottle in the sampling line (see Fig. 1).

Sample ID	BaSO ₄ Rec mg	$\delta^{34}\text{S}$ ‰	$\Delta^{33}\text{S}$ ‰
O ₃ -1	2.8	16.0	-0.170
O ₃ -3	392.8	10.4	-0.072
O ₃ -UV-1	26.1	8.7	0.296
O ₃ -UV-3	63.7	12.6	-0.063
O ₃ - γ -1	19.4	13.9	-0.041
O ₃ -UV- γ -1	16.8	9.7	0.232

carried by N₂(g), washed through a water trap, and reacted with a 0.1 M AgNO₃ solution to convert it into Ag₂S. The Ag₂S was then converted into SF₆ by reaction with excess F₂ at 200 °C in a nickel reaction tube and then purified by gas chromatography using a technique similar to that of Ono et al. (2006). Additionally a separate setup with an improved purification system was used to analyze the samples for ³⁶S with better precision. The isotopic composition of SF₆ was determined using a Finnigan MAT 253 mass spectrometer (Thermo Fishier Scientific) equipped with a dual inlet system. The SF₅⁺ ions with mass 127, 128, 129, and 131 amu were measured, corresponding to ³²S, ³³S, ³⁴S, and ³⁶S.

3 Results and discussion

The results of the analysis are presented in Table 1. Columns three and four of the table show $\delta^{34}\text{S}$ and $\Delta^{33}\text{S}$ for all samples. Data for $\Delta^{36}\text{S}$ was also measured and is presented in Appendix A. The fractionation data of $\delta^{34}\text{S}$ and $\Delta^{33}\text{S}$ is presented graphically in Fig. 2. Definitions for the isotopic designations are given in Appendix B.

3.1 Sulphate production

The sulphate mass obtained from each bottle is listed in the second column of Table 1. Sulphate is generated in the setup in all different operation modes and yields vary widely – for instance more sulphuric acid is formed with UV light present than for the gamma source but the sources combined yield less than each individual source. Seeing sulphate in the samples where UV and gamma radiation was not used indicates a process occurring in the trapping bottles themselves. The experiment without ozone, which showed no precipitation, strongly indicates that this process is liquid phase oxidation of SO₂ by ozone where the reactants become dissolved in the liquid phase depending on their Henry's Law constants,

leading to the conversion of SO₂ to H₂SO₄ and not simply dissolved SO₂ precipitating as BaSO₃. Note that the yields in the experiment without UV and gamma radiation increased for each bottle counting from the chamber and that the isotopic signature of this material is consistent with oxidation of SO₂ by O₃. In the experiment with UV and the experiment with gamma there was more sample in the third bottle than in the second but also more in the first than in the second, indicating that two processes were taking place.

We conclude that while the liquid phase ozone oxidation process takes place in all experiments, the amount of sulphate produced via this process should be small in the first bottle, compared to the amount produced in experiments that had other formation processes present. The effect of the aqueous oxidation process on $\delta^{34}\text{S}$ in the first bottle will thus be small since the amount produced by the gas phase processes are larger (see Tab. 1 for a comparison of the sample masses recovered). Additionally the concentration of ozone is substantially smaller (about half) in the UV experiments, due to photolysis.

3.2 ³⁴S

The $\delta^{34}\text{S}$ values of our sample O₃-UV-1 (8.7 ± 0.4 ‰) can be compared to the recently published values by Harris et al. (2012) for the OH reaction. In the Harris et al. study and this work, UV photolysis was used to generate OH via ozone photolysis, in the first case prior to the reaction chamber but in the second case within the reaction chamber – see Sect. 3.3. Their $^{34}\alpha$ value of 1.0077 ± 0.0022 at 30 °C is easily converted to our $\delta^{34}\text{S}$ notation by subtracting 1, giving 7.7 ± 2.2 ‰, which appears to agree with our result. The $\delta^{34}\text{S}$ of the OH reaction has also been estimated by Leung et al. (2001), using RRKM transition-state theory and by Tanaka et al. (1994) using ab initio calculations. They do, however, arrive at very different values: 140 and -9.0‰, respectively. While the Leung et al. result shows enrichment in ³⁴S, as in this study, the effect is much larger than what we measure.

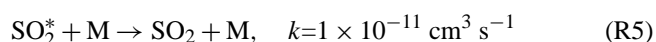
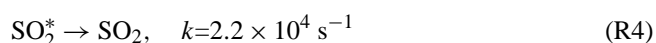
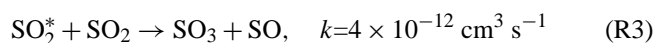
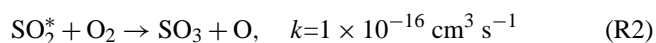
Harris et al. (2012) also measured liquid phase oxidation, but it is not obvious that we can make a direct comparison to our experiments without UV and gamma radiation. It is clear that not all sulphuric acid is collected in the first bottle in the line as we get more material in the second and third bottles and thus it is not possible to distinguish the fractionation for the liquid phase process. However we note that the $\delta^{34}\text{S}$ value for our sample O₃-1 (16.0 ± 0.4 ‰) agrees with the value at 22 °C from the Harris et al. (2012) study of 14.8 ± 2.7 ‰. The Harris et al. (2012) results are also shown in Fig. 2. Note that Harris et al. (2012) find a $\Delta^{33}\text{S}$ value of ~ 8 ‰ for the SO₂ + O₃ reaction, but this “may be a measurement artefact as only two samples were measured” (Harris et al., 2012). Also, their reported uncertainties for the ³³S values of the SO₂ + OH reaction are quite large due to counting statistics. Therefore we report their data in Fig. 2 with errors on the $\Delta^{33}\text{S}$ scale exceeding the depicted y-axis.

The samples O₃-1 and O₃-3 show a difference in $\delta^{34}\text{S}$ which can be explained by the isotopic composition of the substrate of the bottles which differs when operated in series, i.e. the first bottle leaves depleted substrate to be trapped in later bottles, so that $\delta^{34}\text{S}$ values are shifted to lower numbers.

The isotopic mixing line in Fig. 2 shows the basic fractionation present in all samples from the ozone process towards the fractionation for the other processes. Following the mixing line we note that the values of both $\delta^{34}\text{S}$ and $\Delta^{33}\text{S}$ of sample O₃-UV- γ -1 lie between the values for samples O₃-UV-1 and O₃- γ -1, indicating that in this case both processes are happening at the same time. Assuming that sample O₃-UV- γ -1 is a combination of the two processes, we find, using a linear combination of the $\delta^{34}\text{S}$ values, that 79 % of sample O₃-UV- γ -1 originates from the UV process and 21 % from the γ process, ignoring ozone oxidation.

3.3 Non-mass dependent fractionation ($\Delta^{33}\text{S}$)

NMD was observed in our samples, especially for the UV experiment (O₃-UV-1). This stands in contrast to the mass dependent signal reported by Harris et al. (2012), however their sensitivity to ^{33}S is not very high and their experiment was not directly irradiated with UV. NMD signals in SO₂ mainly arise from differences in the absorption spectra of isotopologues (Danielache et al., 2008) and in this experiment the reaction volume, which contains a high SO₂ concentration (0.01 %), is directly exposed to light at 253.65 nm, which was not the case in the Harris et al. experiment. These conditions make a host of new reactions possible (Ueno et al., 2009), the most important ones being



Note that SO₂^{*} can denote both a singlet and triplet state, where the singlet can be relaxed into the triplet state. The shown reaction rates are for the singlet state but similar relations occur for the triplet. The absorption cross section for SO₂ at 253.65 nm is $\sim 1 \times 10^{-19} \text{ cm}^2$ (Danielache et al., 2008), and the concentration of SO₂ is 0.01 %. The ozone cross section is $\sim 1 \times 10^{-17} \text{ cm}^2$ at 253.65 nm and we have ~ 400 ppb ozone in the reaction volume. At 40–45 % RH, 0.2 of each O(¹D) from Eq. (R7) (Appendix C) becomes OH (Seinfeld and Pandis, 2006, chap. 6) – the remaining O(¹D) is quenched back to the ground state O(³P). The photon flux and pathlength for the light is the same in both cases so relative to each other we have $1 \times 10^{-19} \text{ cm}^2 \times 1 \times 10^{-4} = 1 \times 10^{-23} \text{ cm}^2$ for the SO₂ excitation pathway and $1 \times 10^{-17} \text{ cm}^2 \times 4 \times 10^{-7} \times 0.2 = 8 \times$

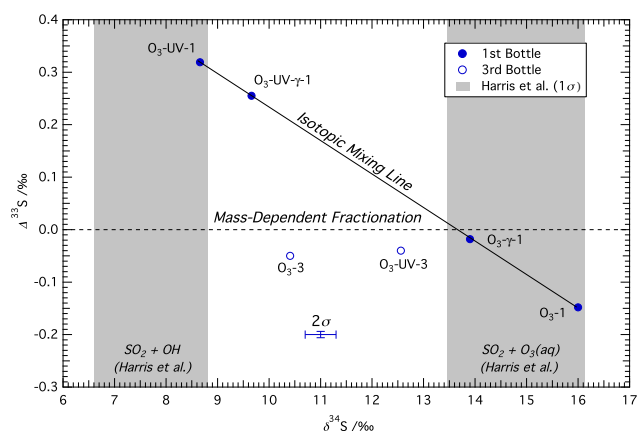


Fig. 2. $\delta^{34}\text{S}$ and $\Delta^{33}\text{S}$ for the analyzed samples, taken from Table 1. Labels show the sample ID. Also shown are the 2σ error bars in the $\delta^{34}\text{S}$ and $\Delta^{33}\text{S}$ axes. The value for the OH and O₃(aq) reactions from Harris et al. (2012) are also shown in grey (width: 1σ). The line indicates the mixing of different production processes and their resulting isotopic composition.

10^{-25} cm^2 for ozone. This slightly favours the excitation pathway, starting with Reaction (R1). However, the excited SO₂^{*} can easily be relaxed back to the ground state before it is oxidised to SO₃. With 0.01 % SO₂ Reaction (R2) is the quickest pathway to SO₃ of Reactions (R2) and (R3), but the quenching reaction, Reaction (R5), is faster still, meaning that most of the excited SO₂ should be relaxed back to the ground state before reacting further, even at these highly elevated concentrations of SO₂.

Using the high resolution spectra obtained by Danielache et al. (2008) we can make an estimate of the expected NMD signal due to photo-excitation. Using the cross section at 253.65 nm, we predict a $\Delta^{33}\text{S}$ of 18.3 to 24.7 ‰ for SO₂^{*} compared to SO₂ depending on the linewidth of the excitation source. Using more recent data (Danielache et al., 2012) we get 13.5–36.0 ‰. Since we only have a small conversion of our SO₂ reservoir this can be compared directly to our measured $\Delta^{33}\text{S}$ of 0.30 ‰. This shows that the measured NMD can be explained by photo-excitation. Our $\delta^{34}\text{S}$ result is thus obtained from a combination of the OH reaction and the UV excitation reaction. However, since our measured $\Delta^{33}\text{S}$ is so small compared to the value expected from the excitation pathway most of the sulphuric acid production in the UV experiments most likely proceeds by the OH pathway and thus justifies comparison with the results of Harris et al. (2012). Furthermore the lack of NMD in sample O₃-UV-3 is due to the liquid phase oxidation dominating.

A different study by Farquhar et al. (2001) focused on NMD signals in SO₂ photolysis reactions and described systems with different light sources. Comparing our data to theirs shows the same trends (our lamp compares best, but not perfectly, to their KrF excimer laser), but one has to keep in mind that minute changes in the irradiance

may shift isotopic effects drastically (Danielache et al., 2008). Nevertheless, the $\Delta^{36}\text{S}$ values reported here (see Appendix A) are pointing towards the negative, while the $\Delta^{33}\text{S}$ values show a positive trend, just as in the Farquhar et al. (2001) study.

A small non-zero $\Delta^{33}\text{S}$ is seen in samples O₃-3, O₃-UV-3, and O₃- γ -1, while sample O₃-1 has a stronger signal. They are all significant with respect to the error, but we do not have a full understanding of the underlying process. In order to understand this effect a model of the heterogeneous reaction could be constructed similar to the sulphate reduction model of Rees (1973) (see also Johnston, 2011).

3.4 Gamma experiments

Ionising radiation gives energy to the electron clouds in molecules often generating ion pairs:



In our experiment, as well as the atmosphere, M is typically N₂. The resulting electrons eventually attach to molecules, depending on their electron affinity and concentrations. Oxygen and nitrogen exist in the greatest abundance and since oxygen has a positive electron affinity the O₂⁻ ion is spontaneously formed. The core ion then attracts water to form hydrated clusters, such as O₂⁻(H₂O)_n – this happens even at otherwise unsaturated conditions, due to the electric charge. There are many options for further reaction – one relevant scheme is presented by Bork et al. (2011a,b). In the troposphere ionisation is mostly caused by secondary particles (muons and electrons) formed by galactic cosmic rays with energies >1 GeV (Bazilevskaya et al., 2008). Although the energy of the gamma source (662 keV) is somewhat lower than that of cosmic rays penetrating the lower atmosphere the ions produced are the same. Based on the difference in $\delta^{34}\text{S}$, the mechanism for sulphate formation in the gamma reaction is clearly different from the OH oxidation pathway. The amount produced is also too high to be explained by this mechanism. The estimated OH production per ionisation is about 2 (Müller and Crutzen, 1993) and the ionisation in our chamber is estimated to be 1000 cm⁻³ s⁻¹ (based on a simple model using the activity of the source and distance from the chamber to calculate the energy deposited in the volume), resulting in 6 × 10¹³ OH molecules formed during a run of one week, which would give 23 ng of BaSO₄, orders of magnitude less than the 19.4 mg collected, even if a small part of this comes from the liquid phase oxidation process. The gamma induced fractionation pattern resembles that of the experiments without UV and gamma radiation more even if they are some standard deviations apart, but in the gamma experiment we see much more material in the first bottle than in the following, the reverse pattern of what is seen in the experiments without UV and gamma radiation. This suggests that the mechanism of the gamma pathway is gas-phase or heterogenous chemistry in the chamber and by a mechanism

that somehow enhances the yield far beyond one sulphate per ionisation. That we see a small NMD effect also suggests a chemical pathway. One possible explanation is the mechanism under investigation in Bork et al. (2011a,b) where hydrated ion clusters (Zatula et al., 2011), such as described above, serve as nanoreactors for sulphur oxidation by a process similar to the oxidation of SO₂ by ozone observed in the experiments without UV and gamma radiation.

These experiments clearly suggest that ions may catalyse SO₂ oxidation. However, any ion catalysed mechanism will terminate with collision with OH or another radical since most radicals have high electron affinities, i.e. can form stable anions. In other words, the electron becomes chemically immobilized. In this experiment the dominant electron scavenger is OH. The contribution is thus dependent on the ratio of SO₂ to OH and the ion production rate and we note that in these experiments, the relative concentration of SO₂ to OH was much larger than in the atmosphere. The ion induced contribution should be compared to the oxidation of SO₂ by OH. The third-order rate constant for this reaction is about 4.5 × 10⁻³¹ cm⁶ s⁻¹ (Seinfeld and Pandis, 2006, Appendix B). The gamma-induced pathway scales with $P_{\text{ion}} \cdot [\text{SO}_2]/[\text{OH}]$, where P_{ion} is the ion production rate. The UV pathway scales with $[\text{SO}_2] \cdot [\text{OH}] \cdot M \cdot k$, where k is the rate constant. Since both pathways scale with $[\text{SO}_2]$ the relative contribution of the ion mechanism to the UV mechanism does not depend on $[\text{SO}_2]$. On the other hand it depends on $[\text{OH}]^2$ and on the ion production rate. Thus the relative contribution can vary greatly and will be larger at night when there is little or no OH available. For a daytime $[\text{OH}]$ of e.g. 2 × 10⁶ cm⁻³ and an ion production rate of 4 cm⁻³ s⁻¹ the relative contribution will be 9%. This is of course a very rough estimate and a definitive answer will require further research, such as has been started by Bork et al. (2011b).

4 Conclusions

In this study we investigated the production of sulphuric acid from SO₂ through a number of different pathways. The sulphuric acid was produced using standard gas phase oxidation by OH radicals from ozone photolysis, liquid phase oxidation by ozone, and oxidation initiated by gamma rays. The distributions of stable sulphur isotopes in the products and substrate were measured using isotope ratio mass spectrometry. All methods produced sulphate enriched in ³⁴S and we find a $\delta^{34}\text{S}$ value of 8.7 ± 0.4 ‰ (1 standard deviation) for the UV-initiated OH reaction. Only the experiment with UV light (Hg emission at 253.65 nm) produced a clear non-mass-dependent excess of ³³S of around 0.3 ‰, resulting from a small contribution from photo-excitation. Our results for UV photolysis and possibly aqueous oxidation by ozone, matched isotope patterns seen in earlier measurements. However, these UV photolysis result do not agree with theoretical

Table A1. *Isotopic composition of samples.* The table displays the sample ID, $\Delta^{36}\text{S}$ (normalized against the references as defined in Appendix B), the mass of BaSO_4 used, the mass of Ag_2S recovered, the mass of Ag_2S used, and the amount of SF_6 recovered.

Sample ID	$\Delta^{36}\text{S}$ ‰	BaSO_4 Used mg	Ag_2S Rec mg	Ag_2S Used mg	SF_6 μmol
O ₃ -1	0.5	–	0.689	0.689	2.85
O ₃ -3	0.4	8.99	8.84	2.07	7.91
O ₃ -UV-1	–1.3	–	–	–	6.98
O ₃ -UV-3	0.2	9.39	9.48	2.00	8.87
O ₃ - γ -1	0.1*	5.51	5.09	2.21	9.45
O ₃ -UV- γ -1	–1.0	7.90	7.34	2.13	9.80

* This sample was not measured with the improved purification system.

studies (Tanaka et al., 1994; Leung et al., 2001), suggesting that additional theoretical work is needed.

The pattern of isotopic enrichment produced by gamma rays was distinctly different from that caused by the UV light and similar, but not equal, to that produced by the aqueous oxidation of SO_2 . This, combined with the relative yields of the experiments, suggests a mechanism by which ionising radiation may lead to hydrated ion clusters that serve as nanoreactors for S(IV) to S(VI) conversion.

Appendix A

$\Delta^{36}\text{S}$

In addition to $\delta^{34}\text{S}$ and $\Delta^{33}\text{S}$ we also measured $\Delta^{36}\text{S}$, using an improved purification system for most of the samples. The values can be seen in Table A1. We refrain from going into a detailed analysis of this data but note that the linear relation between $\Delta^{33}\text{S}$ and $\Delta^{36}\text{S}$ is consistent with the isotope mixing shown in Fig. 2. Additionally, Table A1 displays further information on the amount of material used and recovered during the isotopic analysis.

Appendix B

Definitions

Sulphur isotopic compositions are reported as $\delta^{34}\text{S}$ and $\Delta^{33/36}\text{S}$ values normalized against the mean value of our two SO_2 references:

$$\delta^{34}\text{S} = \frac{i R_{\text{sample}}}{i R_{\text{reference}}} - 1$$

where R denotes the isotope ratios ($\frac{34\text{S}}{32\text{S}}$) of samples and reference.

$$\Delta^{33}\text{S} = \delta^{33}\text{S} - [(\delta^{34}\text{S} + 1)^{0.515} - 1]$$

$$\Delta^{36}\text{S} = \delta^{36}\text{S} - [(\delta^{34}\text{S} + 1)^{1.90} - 1]$$

The Δ notation describes the excess or deficiency of ^{33}S and ^{36}S relative to the reference mass-dependent fractionation array (Farquhar et al., 2000b). The Δ values are thus a measure of Non Mass Dependent fractionation (NMD).

The precision based on replicated analysis of Ag_2S standards (IAEA-S1 and in-house Ag_2S) is typically ± 0.3 and ± 0.006 ‰ (1 standard deviation) for $\delta^{34}\text{S}$ and $\Delta^{33}\text{S}$. For $\Delta^{36}\text{S}$ the standard deviation is 0.7 ‰ for the method used to measure the other isotopes and 0.1 ‰ for the improved method. Measurements of the two SO_2 reference samples are close to the stated precisions, suggesting that errors originating from sample handling are minor.

Appendix C

Gas-phase oxidation of SO_2 by OH

Here we list the reactions relevant to the oxidation of SO_2 by OH in the chamber.



Supplementary material related to this article is available online at: <http://www.atmos-chem-phys.net/12/5319/2012/acp-12-5319-2012-supplement.pdf>.

Acknowledgements. This work was supported by the Global Environment Research Fund (A-0904) of the Ministry of the Environment, and Grant-in-Aid for Scientific Research (S-23224013), The Ministry of Education, Culture, Sports, Science and Technology (MEXT), Japan. We thank the IntraMIF network sponsored by the European Community's Seventh Framework Programme (FP7/2007-2013) under grant agreement number 237890 for support. Martin B. Enghoff acknowledges the Carlsberg Foundation and The Danish Council for Independent Research | Natural Sciences for financial support. Shohei Hattori is supported by Grant in Aid for JSPS Research Fellows (DC1, No. 22-7563) and Global COE program Earth to Earths of MEXT, Japan. Yuichiro Ueno is supported by the NEXT program of MEXT, Japan. Nicolai Bork is supported by the Villum foundation.

Edited by: J. B. Burkholder

References

- Bao, H., Rumble, D., and Lowe, D. R.: The five stable isotope compositions of Fig Tree barites: Implications on sulfur cycle in ca. 3.2 Ga oceans, *Geochim. Cosmochim. Ac.*, 71, 4868–4879, doi:10.1016/j.gca.2007.05.032, 2007.
- Baroni, M., Thiemens, M., Delmas, R., and Savarino, J.: Mass-Independent Sulfur Isotopic Compositions in Stratospheric Volcanic Eruptions, *Science*, 315, 84–87, doi:10.1126/science.1131754, 2007.
- Bazilevskaya, G. A., Usoskin, I. G., Flueckiger, E. O., Harrison, R. G., Desorgher, L., Buetikofer, R., Krainev, M. B., Makhmutov, V. S., Stozhkov, Y. I., Svirzhevskaya, A. K., Svirzhevsky, N. S., and Kovaltsov, G. A.: Cosmic ray induced ion production in the atmosphere, *Space Sci. Rev.*, 137, 149–173, doi:10.1007/s11214-008-9339-y, 2008.
- Berndt, T., Böge, O., and Stratmann, F.: Formation of atmospheric $\text{H}_2\text{SO}_4/\text{H}_2\text{O}$ particles in the absence of organics: A laboratory study, *Geophys. Res. Lett.*, 33, L15817, doi:10.1029/2006GL026660, 2006.
- Bork, N., Kurtén, T., Enghoff, M. B., Pedersen, J. O. P., Mikkelsen, K. V., and Svensmark, H.: Ab initio studies of $\text{O}_2^-(\text{H}_2\text{O})_n$ and $\text{O}_3^-(\text{H}_2\text{O})_n$ anionic molecular clusters, $n \leq 12$, *Atmos. Chem. Phys.*, 11, 7133–7142, doi:10.5194/acp-11-7133-2011, 2011a.
- Bork, N., Kurtén, T., Enghoff, M. B., Pedersen, J. O. P., Mikkelsen, K. V., and Svensmark, H.: Structures and reaction rates of the gaseous oxidation of SO_2 by an $\text{O}_3^-(\text{H}_2\text{O})_{0-5}$ cluster – a density functional theory investigation, *Atmos. Chem. Phys.*, 12, 3639–3652, doi:10.5194/acpd-11-29647-2011, 2011b.
- Boy, M., Kulmala, M., Ruuskanen, T. M., Pihlatie, M., Reissell, A., Aalto, P. P., Keronen, P., Dal Maso, M., Hellen, H., Hakola, H., Jansson, R., Hanke, M., and Arnold, F.: Sulphuric acid closure and contribution to nucleation mode particle growth, *Atmos. Chem. Phys.*, 5, 863–878, doi:10.5194/acp-5-863-2005, 2005.
- Brenninkmeijer, C. A. M., Janssen, C., Kaiser, J., Röckmann, T., Rhee, T. S., and Assonov, S. S.: Isotope Effects in the Chemistry of Atmospheric Trace Compounds, *Chem. Rev.*, 103, 5125–5162, doi:10.1021/cr020644k, 2003.
- Curtius, J.: Nucleation of atmospheric aerosol particles, *CR Phys.*, 7, 1027–1045, doi:10.1016/j.crhy.2006.10.018, 2006.
- Danielache, S. O., Hattori, S., Johnson, M. S., Ueno, Y., Nanbu, S., and Yoshida, N.: Photoabsorption cross-section measurements of ^{32}S , ^{33}S , ^{34}S and ^{36}S sulfur dioxide for the B1B1-X1A1 absorption band, *J. Geophys. Res.*, submitted, 2012.
- Danielache, S. O., Eskebjerg, C., Johnson, M. S., Ueno, Y., and Yoshida, N.: High-precision spectroscopy of ^{32}S , ^{33}S , and ^{34}S sulfur dioxide: Ultraviolet absorption cross sections and isotope effects, *J. Geophys. Res.*, 113, D17314, doi:10.1029/2007JD009695, 2008.
- Enghoff, M. B. and Svensmark, H.: The role of atmospheric ions in aerosol nucleation – a review, *Atmos. Chem. Phys.*, 8, 4911–4923, doi:10.5194/acp-8-4911-2008, 2008.
- Enghoff, M. B., Pedersen, J. O. P., Bondo, T., Johnson, M. S., Paling, S., and Svensmark, H.: Evidence for the Role of Ions in Aerosol Nucleation, *J. Phys. Chem. A*, 112, 10305–10309, doi:10.1021/jp806852d, 2008.
- Farquhar, J., Bao, H., and Thiemens, M.: Atmospheric Influence of Earth's Earliest Sulfur Cycle, *Science*, 289, 756–758, doi:10.1126/science.289.5480.756, 2000a.
- Farquhar, J., Jackson, T. L., and Thiemens, M. H.: A ^{33}S enrichment in ureilite meteorites: Evidence for a nebular sulfur component, *Geochim. Cosmochim. Ac.*, 64, 1819–1825, doi:10.1016/S0016-7037(00)00356-2, 2000b.
- Farquhar, J., Savarino, J., Airieau, S., and Thiemens, M. H.: Observation of wavelength-sensitive mass-independent sulfur isotope effects during SO_2 photolysis: Implications for the early atmosphere, *J. Geophys. Res.*, 106, 32829–32839, doi:10.1029/2000JE001437, 2001.
- Fehsenfeld, F. C. and Ferguson, E. E.: Laboratory studies of negative ion reactions with atmospheric trace constituents, *J. Chem. Phys.*, 61, 3181–3193, doi:10.1063/1.1682474, 1974.
- Forster, P., Ramaswamy, V., Artaxo, P., Berntsen, T., Betts, R., Fahey, D. W., Haywood, J., Lean, J., Lowe, D. C., Myhre, G., Nganga, J., Prinn, R., Raga, G., Schulz, M., and Van Dorland, R.: Changes in Atmospheric Constituents and in Radiative Forcing, in: *Climate Change 2007: The Physical Science Basis. Contribution of Working Group I to the Fourth Assessment Report of the Intergovernmental Panel on Climate Change*, edited by: Solomon, S., Qin, D., Manning, M., Chen, Z., Marquis, M., Averyt, K. B., Tignor, M., and Miller, H. L., Cambridge University Press, 2007.
- Gao, Y. Q. and Marcus, R. A.: Strange and Unconventional Isotope Effects in Ozone Formation, *Science*, 293, 259–263, doi:10.1126/science.1058528, 2001.
- Guo, Z., Li, Z., Farquhar, J., Kaufman, A. J., Wu, N., Li, C., Dickerson, R. R., and Wang, P.: Identification of sources and formation processes of atmospheric sulfate by sulfur isotope and scanning electron microscope measurements, *J. Geophys. Res.*, 115, D00K07, doi:10.1029/2009JD012893, 2010.
- Harris, E., Sinha, B., Hoppe, P., Crowley, J. N., Ono, S., and Foley, S.: Sulfur isotope fractionation during oxidation of sulfur dioxide: gas-phase oxidation by OH radicals and aqueous oxidation by H_2O_2 , O_3 and iron catalysis, *Atmos. Chem. Phys.*, 12, 407–424, doi:10.5194/acp-12-407-2012, 2012.
- Hirsikko, A., Nieminen, T., Gagne, S., Lehtipalo, K., Manninen, H. E., Ehn, M., Horrak, U., Kerminen, V.-M., Laakso, L., McMurry, P. H., Mirme, A., Mirme, S., Petaja, T., Tammet, H., Vakkari, V., Vana, M., and Kulmala, M.: Atmospheric ions and nucleation: a review of observations, *Atmos. Chem. Phys.*, 11, 767–798, doi:10.5194/acp-11-767-2011, 2011.
- Jefferson, A., Tanner, D. J., Eisele, F. L., and Berresheim, H.: Sources and sinks of H_2SO_4 in the remote Antarctic marine, *J. Geophys. Res.*, 103, 1639–1645, doi:10.1029/97JD01212, 1998.
- Johnson, M. S., Feilberg, K. L., von Hessberg, P., and Nielsen, O. J.: Isotopic processes in atmospheric chemistry, *Chem. Soc. Rev.*, 31, 313–323, doi:10.1039/b108011n, 2002.
- Johnston, D. T.: Multiple sulfur isotopes and the evolution of Earth's surface sulfur cycle, *Earth-Sci. Rev.*, 106, 161–183, doi:10.1016/j.earscirev.2011.02.003, 2011.
- Kazil, J., Harrison, R. G., and Lovejoy, E. R.: Tropospheric New Particle Formation and the Role of Ions, *Space Sci. Rev.*, 137, 241–255, doi:10.1007/s11214-008-9388-2, 2008.
- Kirkby, J., Curtius, J., Almeida, J., Dunne, E., Duplissy, J., Ehrhart, S., Franchin, A., Gagne, S., Ickes, L., Kuerten, A., Kupc, A., Metzger, A., Riccobono, F., Rondo, L., Schobesberger, S., Tsagkogeorgas, G., Wimmer, D., Amorim, A., Bianchi, F., Breitenlechner, M., David, A., Dommen, J., Downard, A., Ehn, M., Flagan, R. C., Haider, S., Hansel, A., Hauser, D., Jud, W., Jun-

- ninen, H., Kreissl, F., Kvashin, A., Laaksonen, A., Lehtipalo, K., Lima, J., Lovejoy, E. R., Makhmutov, V., Mathot, S., Mikkilä, J., Minginette, P., Mogo, S., Nieminen, T., Onnela, A., Pereira, P., Petaja, T., Schnitzhofer, R., Seinfeld, J. H., Sipila, M., Stozhkov, Y., Stratmann, F., Tome, A., Vanhanen, J., Viisanen, Y., Vrtala, A., Wagner, P. E., Walther, H., Weingartner, E., Wex, H., Winkler, P. M., Carslaw, K. S., Worsnop, D. R., Baltensperger, U., and Kulmala, M.: Role of sulphuric acid, ammonia and galactic cosmic rays in atmospheric aerosol nucleation, *Nature*, 476, 429–433, doi:10.1038/nature10343, 2011.
- Kulmala, M.: How Particles Nucleate and Grow, *Science*, 202, 1000–1001, doi:10.1126/science.1090848, 2003.
- Kurtén, T., Loukonen, V., Vehkamäki, H., and Kulmala, M.: Amines are likely to enhance neutral and ion-induced sulfuric acid-water nucleation in the atmosphere more effectively than ammonia, *Atmos. Chem. Phys.*, 8, 4095–4103, doi:10.5194/acp-8-4095-2008, 2008.
- Leung, F. Y., Colussi, A. J., and Hoffmann, M. R.: Sulfur isotopic fractionation in the gas-phase oxidation of sulfur dioxide initiated by hydroxyl radicals, *J. Phys. Chem. A*, 105, 8073–8076, doi:10.1021/jp011014+, 2001.
- Lovejoy, E. R., Curtius, J., and Froyd, K. D.: Atmospheric ion-induced nucleation of sulfuric acid and water, *J. Geophys. Res.*, 109, 1–11, doi:10.1029/2003JD004460, 2004.
- Manninen, H. E., Nieminen, T., Asmi, E., Gagne, S., Hakkinen, S., Lehtipalo, K., Aalto, P., Vana, M., Mirme, A., Mirme, S., Horrak, U., Plass-Duelmer, C., Stange, G., Kiss, G., Hoffer, A., Toeroe, N., Moerman, M., Henzing, B., de Leeuw, G., Brinkenberg, M., Kouvarakis, G. N., Bougiatioti, A., Mihalopoulos, N., O'Dowd, C., Ceburnis, D., Arneth, A., Svenningsson, B., Swietlicki, E., Tarozzi, L., Decesari, S., Facchini, M. C., Birmili, W., Sonntag, A., Wiedensohler, A., Boulon, J., Sellegri, K., Laj, P., Gysel, M., Bukowiecki, N., Weingartner, E., Wehrle, G., Laaksonen, A., Hamed, A., Joutsensaari, J., Petaja, T., Kerminen, V. M., and Kulmala, M.: EUCAARI ion spectrometer measurements at 12 European sites – analysis of new particle formation events, *Atmos. Chem. Phys.*, 10, 7907–7927, doi:10.5194/acp-10-7907-2010, 2010.
- Müller, R. and Crutzen, P. J.: A Possible Role of Galactic Cosmic Rays in Chlorine Activation During Polar Night, *J. Geophys. Res.*, 98, 20483–20490, doi:10.1029/93JD02455, 1993.
- Ono, S., Eigenbrode, J. L., Pavlov, A. A., Kharecha, P., Rumble III, D., Kasting, J. F., and Freeman, K. H.: New insights into Archean sulfur cycle from mass-independent sulfur isotope records from the Hamersley Basin, Australia, *Earth Planet. Sc. Lett.*, 213, 15–30, doi:10.1016/S0012-821X(03)00295-4, 2003.
- Ono, S., Wing, B., Johnston, D., Farquhar, J., and Rumble, D.: Mass-dependent fractionation of quadruple stable sulfur isotope system as a new tracer of sulfur biogeochemical cycles, *Geochim. Cosmochim. Ac.*, 70, 2238–2252, doi:10.1016/j.gca.2006.01.022, 2006.
- Pavlov, A. A., Mills, M. J., and Toon, O. B.: Mystery of the volcanic mass-independent sulfur isotope fractionation signature in the Antarctic ice core, *Geophys. Res. Lett.*, 32, L12816, doi:10.1029/2005GL022784, 2008.
- Raes, F., Janssens, A., and Eggermont, G.: A synergism between ultraviolet and gamma radiation in producing aerosol particles from SO₂–H₂SO₄ laden atmospheres, *Atmos. Environ.*, 19, 1069–1073, doi:10.1016/0004-6981(85)90191-X, 1985.
- Rees, C. E.: Steady-state model for sulfur isotope fractionation in bacterial reduction processes, *Geochim. Cosmochim. Ac.*, 37, 1141–1162, doi:10.1016/0016-7037(73)90052-5, 1973.
- Romero, A. B. and Thiemens, M. H.: Mass-independent sulfur isotopic compositions in present-day sulfate aerosols, *J. Geophys. Res.*, 108, 4524, doi:10.1029/2003JD003660, 2003.
- Sakai, H., Des Marais, D. J., Ueda, A., and Moore, J. G.: Concentrations and isotope ratios of carbon, nitrogen and sulfur in ocean-floor basalts, *Geochim. Cosmochim. Ac.*, 48, 2433–2441, doi:10.1016/0016-7037(84)90295-3, 1984.
- Schmidt, J. A., Johnson, M. S., and Schinke, R.: Isotope effects in N₂O photolysis from first principles, *Atmos. Chem. Phys.*, 11, 8965–8975, doi:10.5194/acp-11-8965-2011, 2011.
- Seinfeld, J. H. and Pandis, S. N.: *Atmospheric Chemistry and Physics: From Air Pollution to Climate Change*, Second Edn., John Wiley and Sons, 2006.
- Sipilä, M., Berndt, T., Petaja, T., Brus, D., Vanhanen, J., Stratmann, F., Patokoski, J., Mauldin, III, R. L., Hyvarinen, A.-P., Lihavainen, H., and Kulmala, M.: The Role of Sulfuric Acid in Atmospheric Nucleation, *Science*, 327, 1243–1246, doi:10.1126/science.1180315, 2010.
- Svensmark, H., Pedersen, J. O. P., Marsh, N. D., Enghoff, M. B., and Uggerhøj, U. I.: Experimental evidence for the role of ions in particle nucleation under atmospheric conditions, *P. Roy. Soc. Lond. A Mat.*, 463, 385–396, doi:10.1098/rspa.2006.1773, 2007.
- Tanaka, N., Rye, D. M., Xiao, Y., and Lasag, A. C.: Use of stable sulfur isotope systematics for evaluating oxidation reaction pathways and in-cloud-scavenging of sulfur-dioxide in the atmosphere, *Geophys. Res. Lett.*, 21, 1519–1522, doi:10.1029/94GL00893, 1994.
- Thiemens, M. H.: History and Applications of Mass-Independent Isotope Effects, *Annu. Rev. Earth. Pl. Sc.*, 34, 217–262, doi:10.1146/annurev.earth.34.031405.125026, 2006.
- Ueno, Y., Ono, S., Rumble, D., and Maruyama, S.: Quadruple sulfur isotope analysis of ca. 3.5 Ga Dresser Formation: New evidence for microbial sulfate reduction in the Early Archean, *Geochim. Cosmochim. Ac.*, 72, 5675–5691, doi:10.1016/j.gca.2008.08.026, 2008.
- Ueno, Y., Johnson, M. S., Danielache, S. O., Eskebjerg, C., Pandey, A., and Yoshida, N.: Geological sulfur isotopes indicate elevated OCS in the Archean atmosphere, solving faint young sun paradox, *P. Natl. Acad. Sci. USA*, 106, 14784–14789, doi:10.1073/pnas.0903518106, 2009.
- Yu, F. and Turco, R. P.: Ultrafine aerosol formation via ion-mediated nucleation, *Geophys. Res. Lett.*, 27, 883–886, doi:10.1029/1999GL011151, 2000.
- Yu, F. and Turco, R. P.: From molecular clusters to nanoparticles: Role of ambient ionization in tropospheric aerosol formation, *J. Geophys. Res.*, 106, 4797–4814, doi:10.1029/2000JD900539, 2001.
- Zatula, A. S., Andersson, P. U., Ryding, M. J., and Uggerud, E.: Proton mobility and stability of water clusters containing the bisulfate anion, HSO₄⁻(H₂O)_n, *Phys. Chem. Chem. Phys.*, 13, 13287–13294, doi:10.1039/c1cp21070j, 2011.